Making high resolution positioning independent of scan rates: A feedback approach

Ajit C. Shegaonkar and Srinivasa M. Salapaka

Citation: Appl. Phys. Lett. **91**, 203513 (2007); doi: 10.1063/1.2813025
View online: http://dx.doi.org/10.1063/1.2813025
View Table of Contents: http://apl.aip.org/resource/1/APPLAB/v91/i20
Published by the AIP Publishing LLC.

Additional information on Appl. Phys. Lett.

Journal Homepage: http://apl.aip.org/
Journal Information: http://apl.aip.org/about/about_the_journal
Top downloads: http://apl.aip.org/features/most_downloaded
Information for Authors: http://apl.aip.org/authors

ADVERTISEMENT

Downloaded 17 Sep 2013 to 130.126.139.15. This article is copyrighted as indicated in the abstract. Reuse of AIP content is subject to the terms at: http://apl.aip.org/about/rights_and_permissions

Making high resolution positioning independent of scan rates: A feedback approach

Ajit C. Shegaonkar
Department of Industrial and Enterprise Systems Engineering, University of Illinois at Urbana-Champaign, Urbana-Champaign, Illinois 61801, USA

Srinivasa M. Salapaka[a)]
Department of Mechanical Science and Engineering, University of Illinois at Urbana-Champaign, Urbana-Champaign, Illinois 61801, USA

(Received 21 June 2007; accepted 25 October 2007; published online 14 November 2007)

A feedback paradigm for achieving high resolution positioning for applications requiring repetitive motions such as image scanning in atomic force microscopy (AFM) is presented. The feedback scheme achieves very high resolution by compromising on the bandwidth of the device, even at high speeds, by making the device equivalent to a low bandwidth band pass filter with the central frequency corresponding to scan frequency. Application of this scheme on a flexure based stacked piezoactuated AFM scanner has demonstrated subnanometer resolution enabling atomic scale stick-slip images on mica, impossible otherwise. Experiments at high scan speeds using this scheme improved the positioning resolution by 96%. © *2007 American Institute of Physics*.
[DOI: 10.1063/1.2813025]

A block diagram representing the dynamics of a stacked piezoelectric actuator driven, flexure based single axis scanning stage is described in Fig. 1. The nonlinearities of the actuator and the flexure stage contribute to the mechanical noise of the system and are collectively represented by n_1. The electronic operation of the sensor contributes to the electronic noise, which mainly includes $1/f$ and white noise, and is represented by n_2.

In an open loop operation (Fig. 1), the positioning resolution, which is the smallest motion that can be differentiated from the noise in the system (signal values greater than three times of the standard deviation of noise give a 99.7% confidence in the signal), is determined mainly by the mechanical noise. The mechanical noise mainly consists of the slowly varying drift and creep, which are therefore prominent in slow scans, and the inertial lag at high frequencies, which is prominent in high speed scans. Hysteresis affects the systems at all frequencies and is particularly prominent in repetitive raster scanning. These nonlinear effects of drift, creep, and hysteresis are sensitive to changes in operating conditions such as ambient temperature, residual polarization in piezoactuators, and most importantly the operating point, the reference value on the nonlinear input-output (input voltage versus stage displacement) graph about which stage motions are calibrated. Therefore, including their precise behavior in device models is practically infeasible, and hence they are treated as noise. This mechanical noise precludes subnanometer resolutions in open loop operation for most stack piezoactuated large flexure based positioning systems. In comparison, small single crystal piezodevices, though suffer from the same problems, have nonlinearities which are less sensitive to operating conditions leading to lesser imprecision in models and hence give better resolution.

Feedback based schemes have demonstrated effective compensation for the creep, drift, hysteresis, and inertial lag problems[1] without requiring their precise models. They compensate for the mechanical noise but at the cost of feeding back the relatively smaller electronic noise. Hence, designing the feedback law to limit the effect of additional electronic noise from the sensor is critical.

For better exposition, we present the analysis and design of feedback schemes in terms of *transfer functions*.[2] Transfer function of a system represents the linear dynamics of the system about an operating point. A transfer function block diagram of the scanner in a feedback loop is described in Fig. 2. Moreover, G is the transfer function of the scanner system, comprising of the piezoactuator, the flexure stage, and the sensor, as described in Fig. 1. It represents the dynamical relation between its output, the flexure stage displacement y (which is scaled by a sensor constant), and its input, the voltage u given to the piezoelectric actuator. The relation is denoted by a product operation as $y=Gr$ [or as $y=G(j\omega)r$ when the relation between the Fourier components of frequency ω is emphasized]. The feedback controller K decides the control signal u based on the difference between the sensor reading $y_m=y+n$ and the reference scan trajectory signal r. The closed loop dynamic relation from the reference trajectory r to tracking error r-y is given by the *sensitivity* transfer function $S=1/(1+GK)$, while the *complementary sensitivity* $T=GK/(1+GK)$ represents the transfer function from r to y. The tracking error is given by

$$e = r - y = Sr + Tn. \tag{1}$$

Thus, the tracking error, which is given by the superposition of the error contribution Sr from the reference signal r and the error contribution Tn from the electronic noise n, is ad-

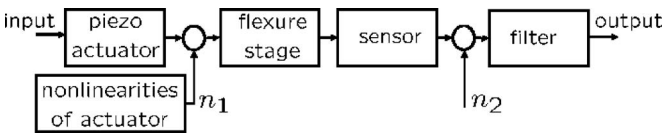

FIG. 1. Single axis open loop. The piezoactuator drives the flexure stage and its movement is measured by a sensor.

[a)]Electronic mail: salapaka@uiuc.edu

 © 2007 American Institute of Physics

Downloaded 17 Sep 2013 to 130.126.139.15. This article is copyrighted as indicated in the abstract. Reuse of AIP content is subject to the terms at: http://apl.aip.org/about/rights_and_permissions

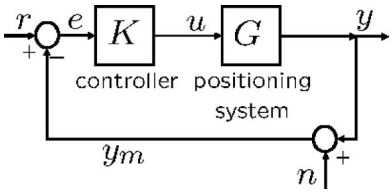

FIG. 2. Closed loop system. Moreover, r is the reference signal, u the control output, y the system output, n the noise (combination of n_1 and n_2), and y_m the measured output.

versely affected by large values of scan range of r and the amplitude of noise n. Thus, high resolution can be achieved by designing the feedback law K such that $S(j\omega)$ and $T(j\omega)$ are small in those frequency ranges where the frequency contents of r and n, respectively, are large. However, there are fundamental restrictions on the design of S and T through K. For instance, at no frequency, $S(j\omega)$ and $T(j\omega)$ can simultaneously be made small since their sum satisfies

$$S(j\omega) + T(j\omega) \equiv 1, \tag{2}$$

at all frequencies ω. Similarly, there is another limitation described by the Bode integral law[3,4] which says that for no design of K, $S(j\omega)$ for stable systems can be made small at all frequencies since $S(j\omega)$ satisfies the following conservation condition:

$$\int_0^\infty \log(|S(j\omega)|)d\omega = 0. \tag{3}$$

In view of these limitations, there is an inherent trade-off between the *positioning resolution* and the *positioning bandwidth* of the device. For a closed loop system, resolution is defined in terms of the standard deviation of the error signal e, and bandwidth of the closed loop system is defined as the rejection frequency range of S; i.e., the frequency range of reference signal over which the overall error due to the reference signal and electronic noise still remains below within the specified accuracy. While trying to reduce the overall error e, the error due to large range of frequency content in reference signal can be made small only at the expense of an increased error due to noise at those frequencies and vice versa. Since the electronic noise has contents in, practically, all the frequencies, obtaining high resolution requires a high rejection bandwidth of T implying a very low rejection bandwidth of S [from Eq. (2)]. Fortunately, for applications such as raster scanning, the range of appreciable frequency content is low (some scans even have only one frequency), thus making it possible to achieve high resolution.

From the design viewpoint, the transfer functions S and T in Eq. (1) are interpreted as filters that act on r and n to give e. Typical designs do not exploit the trade-off between the resolution and bandwidth to achieve high resolution. For example, many designs make S small without making the rejection bandwidth of S small and thus sacrifice resolution. S and T are typically designed as high pass and low pass filters, respectively. For high resolution in low frequency scans (where r has only low-frequency content), this design can be made to exploit the resolution-bandwidth trade-off by making T have a very low pass bandwidth that, from Eq. (2), forces S to have a very low rejection bandwidth resulting in high resolution output. However, this controller does not work for high-frequency-content reference signals, since S is

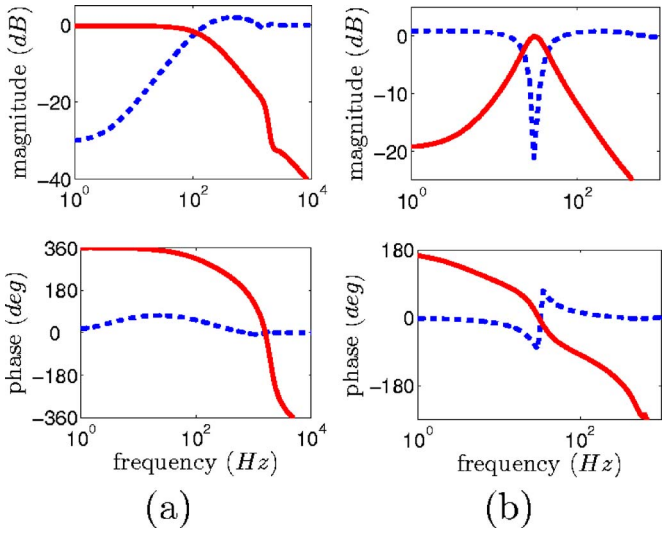

FIG. 3. (Color online) Closed loop transfer functions. (a) Traditional low pass filter T (solid curve) and high pass filter S (dotted curve). (b) The proposed controller design results in a band pass filter T (solid curve) and a band reject filter S (dotted curve), and hence high resolution can be obtained at any speeds of operation by designing the narrow pass and reject band around the operating speed (frequency).

not small at these frequencies. Traditionally, the rejection bandwidth of the resulting closed loop transfer function S is increased so that the system works for higher frequency reference signals [Fig. 3(a)]. However, this results in higher bandwidth of T increasing the error due to noise, and the closed loop system gets a higher bandwidth at the expense of resolution. Here, we propose to design the controller such that S and T have the shapes of band reject and band pass filters, respectively, instead of the traditional high pass and low pass filter designs [Fig. 3(b)]. By keeping the rejection bandwidth of band reject filter S low, the closed loop system achieves very low e and high resolution. In this design, we still have the flexibility of locating the central frequency of the reject band of S (equivalently, the pass band of T) at any desired frequency, which includes high frequencies. Thus, reducing the bandwidth of the closed loop system for achieving high resolution does not necessarily require low speed (frequency) operation. Thus, by designing S with a low rejection bandwidth around the scan frequency, both for low and high frequency scans, we achieve high resolution scanning without any speed limitations. The design of the controllers that achieve these shapes for S and T under constraints, such as in Eqs. (2) and (3), is done using system theoretic tools such as H_∞ optimal control design.[5]

Experimental verification was done on the nanoscanning stage of a commercial AFM, three-dimensional molecular force probe from Asylum Research, Inc., Santa Barbara. Three different results are presented here to bring out the effective high resolution performance capability of the above control paradigm. In the first experiment, mica was imaged over a very small scan range of 6–8 nm (see Fig. 4) at very slow scan rates (0.02 Hz). Under these conditions, the friction signal from mica is expected to show a triangular waveform representing the stick-slip phenomenon[6,7] with a periodicity of 5.2 Å, which can be seen only if the nanoscanning used during imaging has a subnanometer positioning resolution. This result could not be achieved using open loop operation and standard high bandwidth controller for the scan-

Downloaded 17 Sep 2013 to 130.126.139.15. This article is copyrighted as indicated in the abstract. Reuse of AIP content is subject to the terms at: http://apl.aip.org/about/rights_and_permissions

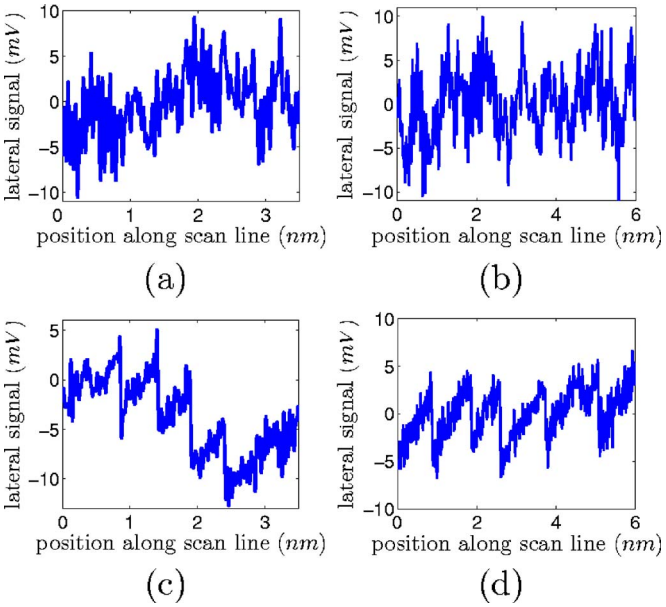

FIG. 4. Lateral force scan line image of mica. (a) and (b) are obtained with a low pass filter T for the positioning axis. (c) and (d) are obtained with a low bandwidth controller for the positioning axis. No stick slip is observed in the friction signal when the controller in (a) and (b) is used for lateral positioning. When the controller in (c) and (d) is used, lateral resolution is very high (subnanometer), and we obtain the expected stick slip periodicity of 5.2 Å in (c) and its multiples in (d).

ning stage. When a very low bandwidth (2.85 Hz) controller was designed for the scanning axis with the complementary sensitivity T as a low pass filter, subnanometer positioning resolution was obtained. This enabled capturing the lattice averaged atomic scale stick-slip phenomenon in the friction signal.

In the second experiment, a very high scan range high speed positioning was done at a frequency of 31.25 Hz. The reference signal and output positioning signal obtained for the long range high speed operation can be seen in Fig. 5. The standard deviation of the tracking error using a traditional controller resulting in a high bandwidth (66.5 Hz) low pass filter T was as high as 3.85 μm for a scan range of 25 μm, whereas the tracking error using a controller resulting in a very low bandwidth (24 Hz) band pass filter shaped closed loop transfer function T, with a zero phase central frequency at 31.25 Hz, was 0.139 μm, an improvement of 96%. This significant improvement in resolution using a very low bandwidth band pass controller with a certain zero phase frequency is because the resulting closed loop system has a zero phase lag at the operating frequency of 31.25 Hz.

As the scan size reduces, the error contribution due to the noise dominates over the error due to the reference signal. The effectiveness of this low bandwidth band pass shaped closed loop transfer function T in rejecting the noise to achieve high resolution can be demonstrated by very low range scans. Hence, the next experiment was done by repeating the second experiment with the scan size kept at zero to

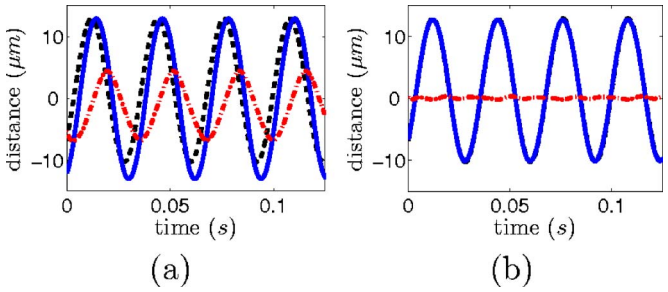

FIG. 5. (Color online) Tracking at 31.25 Hz. (a) High bandwidth controller shows poor tracking at high speeds. Output (dotted curve) cannot follow the reference signal (solid curve) resulting in large errors (dash-dot curve). (b) The band pass controller with low bandwidth but central frequency equal to the high speed of scanning shows excellent tracking with a resolution increasing by 96%.

have a zero error contribution from the reference signal. Hence, the overall error is given by $e=Tn$. Because of the very low pass bandwidth of T, we expect a very low error and, hence, high resolution. However, this cannot be verified directly from the available signals of y_m and e_m as they are good measures of y and e, respectively, only for large scans where the signal to noise ratio is high. Hence, the error e is obtained by taking the product of experimentally obtained T and n. This is done by using the following identity:

$$\mu^2 + \sigma^2 = \int_0^\infty |F(j\omega)|^2 X(\omega) d\omega, \tag{4}$$

which relates the mean μ and standard deviation σ of the output signal y from a filter $F(j\omega)$ (that is, $y=Fx$) in terms of the power spectral density (PSD) $X(\omega)$ of input x.[8] This method is validated by computing the standard deviation of e_m and comparing it with the standard deviation obtained by using Eq. (4) and the experimentally obtained S and the PSD of n. The standard deviations of e_m from both methods were found to be in good agreement with each other, thus justifying the prescribed method. The standard deviation of e obtained from this experimental method was 0.41 nm for the controller used in second experiment as against a value of 1.32 nm obtained when a high bandwidth controller was used, which has a significant improvement of 68.9%.

S.M.S. acknowledges the financial support of NSF Grant No. ECS 0449310 CAR.

[1]D. Croft, G. Shedd, and S. Devasia, *Proceedings of the American Control Conference*, 2000 (unpublished), p. 2123.
[2]J. Bechhoefer, Rev. Mod. Phys. **77**, 783 (2005).
[3]H. Bode, *Network Analysis and Feedback Amplifier Design*, 1st edition (Van Nostrand, New York, 1945).
[4]I. M. Horowitz, *Synthesis of Feedback Systems*, 1st edition (Academic, New York, 1963).
[5]S. Skogestad and I. Postlethwaite, *Multivariable Feedback Control—Analysis and Design*, 2nd edition (Wiley, Hoboken, NJ, 1997).
[6]Y. Sang, M. Dube, and M. Grant, Phys. Rev. Lett. **87**, 174301 (2001).
[7]B. Bhushan, 2nd edition *Handbook of Micro/Nano Tribology* (CRC, Boca Raton, FL, 1999).
[8]C. Heneghan and G. McDarby, Phys. Rev. E **62**, 6103 (2000).

Downloaded 17 Sep 2013 to 130.126.139.15. This article is copyrighted as indicated in the abstract. Reuse of AIP content is subject to the terms at: http://apl.aip.org/about/rights_and_permissions